Luteolin escape mutants of dengue virus map to prM and NS2B and reveal viral plasticity during maturation.

Minhua Peng[a,b], Geng Li[c], Dahai Luo[d], Kitti Wing Ki Chan[a], Wei Zhang[e], Xiaoping Lai[f], Subhash G. Vasudevan[a]*

[a]Program in Emerging Infectious Disease, Duke-NUS Medical School, Singapore

[b]Mathematical Engineering Academy of Chinese Medicine, Guangzhou University of Chinese Medicine, Guangzhou, China

[c]Center for Animal Experiment, Guangzhou University of Chinese Medicine, Guangzhou, China

[d]Lee Kong Chian School of Medicine, Nanyang Technological University, Singapore

[e]School of Pharmaceutical Sciences, Guangzhou University of Chinese Medicine, Guangzhou, China

[f]Guangdong Provincial Key Laboratory of New Drug Development and Research of Chinese Medicine, Guangzhou University of Chinese Medicine, Guangzhou, China

*Corresponding author: Subhash G. Vasudevan, subhash.vasudevan@duke-nus.edu.sg.

Abstract

We previously showed that luteolin, a well-known plant-derived component found in the "heat clearing" class of Traditional Chinese Medicine (TCM) herbs, is an uncompetitive inhibitor (Ki 58.6 μM) of the host proprotein convertase furin, an endoprotease that is required for maturation of flaviviruses in the *trans*-Golgi compartment. Luteolin also weakly inhibited recombinant dengue virus NS2B/NS3 protease (Ki 140.36 μM) non-competitively. In order to further explore the mechanism of inhibition we isolated resistant mutants by continuous passaging of DENV2 in the presence of increasing concentrations of luteolin. Nucleotide sequence analysis of the luteolin-resistant escape mutant revealed amino acid substitutions in the prM (T79R) and NS2B (I114M) genes. These mutations were introduced into a DENV2 infectious clone and tested for replication in Huh-7 cells. Interestingly we found that the replication kinetics of prM T19R-NS2B I114M double-mutant (DM) was similar to wild-type virus (WT). On the other hand the prM T19R single mutant (SM1) was attenuated and the NS2B I114M single mutant (SM2) showed enhanced replication. Time of drug addition assay with luteolin showed that the mutant viruses were able to produce more mature virions than WT in the order DM>SM2>SM1>WT. Exogenous addition of furin to purified immature WT or mutant viruses revealed that luteolin blocked the prM cleavage of WT and SM2 at a similar level. On the other hand the SM1 immature virus showed some cleavage while the DM immature virus revealed efficient furin cleavage of prM even in the presence of 50 uM luteolin. Our findings suggest that luteolin inhibition of furin involves a host/pathogen interface that permits the virus to escape the suppression by mutating key residue that may lead to an altered interface. (283 words)

Keywords: Dengue virus, luteolin, resistant mutant, prM protein, NS2B protein, virus muturation

1. Introduction

Dengue fever is a tropical viral disease caused by the four serotypes of dengue virus (DENV1-4) that are usually transmitted to humans through the bite of a female *Aedes aegypti* mosquito. The incidence of dengue fever has grown dramatically around the world in recent decades. Around 390 million cases of dengue infections occur each year in more than 100 countries in the tropical/sub-tropical regions of the world. Up to 25% of all infections lead to symptomatic illness and has become a leading contributor to hospitalization (Bhatt et al., 2013; Brady et al., 2012) and even death in a small subset of patients especially after secondary infections where the phenomenon of antibody dependent enhancement (ADE) of infection is known to cause more severe disease (Halstead, 2007).

Depending on the degree of cleavage of the 180 copies of precursor membrane (prM) protein on the virion surface, DENV exists either as immature or mature virions (Richter et al., 2014). Immature dengue viral particles display the spiky prM proteins on the virion surface and are non-infectious except via formation of immune complexes with prM antibodies which render them infectious (Rodenhuis-Zybert et al., 2010). The mature infectious virus particles are formed by the cleavage of prM by the host proprotein convertase furin located in the *trans*-Golgi network. Briefly, during infection mature or partially mature DENV enters into the host cell by receptor-mediated endocytosis. The low pH of the host endosomes results in the exposure of the fusion loop motif of the E protein needed for fusion with the host endosomal membrane and promotes rearrangement of the E protein on the virion surface from dimer to trimer (Modis et al., 2004; Seema and Jain, 2005). The viral nucleocapsid containing the single positive-stranded viral genomic RNA (gRNA) of ~11000 bases in length is released into the cytoplasm and translated by host ribosome machinery into a single polyprotein. Co- and post-translational cleavage strongly associated with ER membrane (Garcia-Blanco et al., 2016; Reid et al., 2018) results in the three structural proteins (C, prM, E) needed for virion particle formation and seven nonstructural

proteins (NS1, NS2a, NS2b, NS3, NS4a, NS4b, NS5) that are necessary for viral RNA replication. The immature virion containing the nucleocapsid with newly synthesized RNA buds out from the endoplasmic reticulum and is subsequently transported through the acidic *trans*-Golgi network, where the host protease furin cleaves the 166 amino acid residues long integrated membrane protein prM into 'pr' peptide after residue 91 leaving the ectodomain (residues 92 to 130) and C-terminal transmembrane region (residues 131 to 166) to form the M protein on the mature virion surface (Li et al., 2008). The 'pr' peptide remains bound to virion and once the progeny virion is released from the cell, the 'pr' peptide is dissociated at neutral pH and the virus particle becomes infectious and proceeds to the next cycle of infection (Kuhn et al., 2002).

There are no effective countermeasures against dengue and the only licensed vaccine, Dengvaxia, a tetravalent DENV 1-4 vaccine based on the yellow fever 17-D vaccine back bone (CYD-TDV) that is manufactured by Sanofi Pasteur (Hadinegoro et al., 2015), is not widely accepted due to lack of complete protection against all four serotypes (Aguiar M, 2017). In Asian countries where dengue diseases form a significant public health issue during outbreaks, the patients often turn to herbal remedies such as Traditional Chinese Medicine (TCM) since there are no other medicines that can prevent dengue virus infection. We previously showed that luteolin, a commonly found flavone, isolated from the heat clearing TCM herb *Viola yadoensis Makino*, inhibited DENV maturation through restriction of the cellular proprotein convertase furin (Peng et al., 2017). Furin recognition/cleavage sequence 88-Arg-X-X-Arg↓-91 on prM has some similarity to the consensus site of DENV NS2B/NS3 (Li et al., 2005) in that the P1 residues is an Arg, and luteolin was found to be a weak non-competitive inhibitor.

Since furin is a host target we wanted to address the question if it is an attractive therapeutic target that will not readily lead to escape mutants. In this work we isolated a drug resistant mutant after 10 passages in the presence of increasing concentration of luteolin and found two amino acids substitutions at position 79 of the prM (from Thr to Arg) and at position 114 of the NS2B

(Ile to Met). Given our previous demonstration that luteolin weakly inhibits furin and the viral protease the appearance of the two mutations appeared to concur with the biochemical studies so we examined the impact of the mutations either singly (prM T79R designated as SM1; & the NS2B I114M designated as SM2) or as a double mutant (DM) carrying both mutations in a DENV2 infectious clone. The mutants showed varying replication competence and resistance to luteolin in time of drug addition assays as well as exogenous furin cleavage of immature WT or mutant viruses. Our investigations suggest that luteolin inhibition of furin is achieved probably through modulating binding interface between furin and prM and possible epistatic interaction with NS2B/NS3 that reveal a level of plasticity in the maturation process.

2. Materials and Methods

2.1 Cells, virus and compounds

Huh-7 (hepatocellular carcinoma cells, ATCC) cells were cultured in DMEM medium containing 10 % FBS, 1 % penicillin/streptomycin (P/S) at 37^{o}C in 5 % CO_2. BHK-21 (baby hamster kidney fibroblast cells, ATCC) cells were cultured in RPMI 1640 medium containing 10 % FBS, 1 % P/S, at 37 ^{o}C in 5 % CO_2. C6/36, an *Aedes albopictus* cell line (ATCC), was maintained in RPMI 1640 medium containing 25 mM HEPES, 10 % FBS and 1 % P/S, at 28 ^{o}C in the absence of CO_2.

DENV-2 (TSV01, GenBank accession AY037116) was isolated from a patient in April 1993 in Queensland, Australia (McBride WJH, 1995). DENV-2 (EDEN2, GenBank accession EU081177) were obtained from the Early Dengue infection and outcome (EDEN) study in Singapore (Low et al., 2006). The viruses were grown in C6/36 cells and the supernatants were stored at -80°C. Virus titers were determined by plaque assay on BHK-21 cells.

Luteolin (Purity>95%) was purified and isolated as described previously (Peng et al., 2017).

2.2 Generation and sequencing of DENV-2 resistant to luteolin.

Luteolin resistant DENV2 was obtained by serial passaging of DENV2 TSV01 in Huh-7 cells with gradually increasing concentrations of luteolin. 4×10^5 Huh-7 cells were initially infected with DENV-2 TSV01 at MOI 0.3 (passage 1: P_1) for 1h followed by treatment with 5μM luteolin for 48 h. For subsequent passaging, 1ml of the virus inoculum from the previous passage was used for infection. Luteolin treatment was gradually increased from 5μM to 20μM for resistance selection, with an increment of 5μM after every 3 passages. DENV-2 passaged in 0.1% DMSO (v/v) was included as a mocked-treated control. Reduced luteolin susceptibility (defined as a re-bounce in virus titer similar to mocked-treated control) was determined from the supernatants collected at 48 h post-infection by plaque assay. Viral RNA was extracted from the supernatant of the luteolin-resistant virus passage 10 using QIAamp Viral RNA Mini Kit (Qiagen) according to manufacturer's instructions. cDNA was made using ImpromII Reverse Transcription System (Promega) for full genome sequencing following a previously published protocol (Christenbury et al., 2010). Virus sequencing was performed by Sanger sequencing to determine site-specific mutations in the luteolin-resistant virus passages.

2.3 Recombinant mutant virus construction

The DENV2 full length cDNA clones with specific mutations were constructed by using an infectious cDNA clone of stain DENV2-3295 (GenBank accession: EU081177) as described previously (Tay et al., 2015; Tay et al., 2016; Zhao et al., 2015). Figure 2A shows the schematic representation of the luteolin-resist mutant cDNA clones generation. Briefly, a QuikChange II XL site-directed mutagenesis kit (Stratagene) was used to engineer the PrM T79R or NS2B I114M mutation into the subclone pWSK29 DENV2 fragment 1. The following primers were used for the generation of both mutants: prM:T79R forward (5'-GGGTAACTTATGGGAGATGCACCGCCACAGG-3') and reverse (5'-

CCTGTGGCGGTGCATCTCCCATAAGTTACCC-3') and NS2B:I114M forward (5'-CTTTTTCCCGTGTCAATGCCAATCACGGCAGCTGC-3') and reverse (5'-GCAGCTGCCGTGATTGGCATTGACACGGGAAAAAG-3'). The underlined nucleotide corresponds to the mutation that was being made. Fragment 1 bearing the mutations was ligated into the pWSK29 DENV2 fragment 2+3 using the restriction sites *SphI* and *KpnI* to generate the full length infectious clone. All cDNA constructs were verified by automated DNA sequencing.

2.4 In vitro transcription and replication profiling of mutants

cDNA plasmids were linearized with restriction enzyme *Sac*I and *in vitro* transcribed using the T7 mMESSAGE mMACHINE kit (Ambion) following manufacturer's instructions. 10 μg of the *in vitro* transcribed RNA were transfected into C6/36 cells by electroporation as described previously (Tay et al., 2015) to generate the infectious clone-derived viruses for infection studies. Culture medium from the transfected C6/36 cells was collected on day 7 post-electroporation and passaged once to obtain the P_1 virus stock. Both DENV-2 WT and mutants were titered in BHK-21 cells by plaque assay and stored at -80ºC. For infection assay, 2×10^5 Huh-7 cells were seeded into a 12-well plate and incubated overnight at 37ºC in 5% CO_2. Cells were infected with DENV2 WT and mutants at MOI 1 for 1h. Samples were harvested at 6, 12, 24, 48 h post infection for intracellular viral RNA quantification and plaque titration.

2.5 Time-of-drug-addition assay

Time-of-drug-addition assay were performed as previously described (Peng et al., 2017). Briefly, 2×10^5 Huh-7 cells were infected with DENV2 WT and mutants at a MOI 1 for 1 h. At 12 h p.i, 10 μM of luteolin was added to the infected cells. Samples were collected at 24, 36, 60 h p.i for cellular, extracellular viral RNA and viral titer quantification.

2.6 Immunofluorescence assay

IFA against NS3 protein by anti-NS3 human antibody 3F8, E protein by anti-E mouse antibody 4G2 were performed as previously described (Moreland et al., 2012). IFA images were captured at 20× magnification with an inverted fluorescence microscope (Olympus IX71, Center Valley) and image analysis was performed using ImageJ software (Collins, 2007).

2.7 Western blot analysis

Supernatants from the time-of-drug-addition experiment collected at 60 h p.i were cleared from cell debris by low-speed centrifugation and the virus were pelleted by ultracentrifugation (Optima L-100 XP) at 4ºC in a Beckman type SW41 rotor for 2 h at 32000 rpm. Virions pellets were resuspended in NTE buffer containing 12 mM Tris at pH 8, 120 mM NaCl, and 1 mM EDTA. Subsequently, approximately 10^9 copies of genome-containing virus particles were subjected to electrophoresis by 15% SDS-PAGE gel using 4× non-reducing buffer [0.2 M Tris-HCl (PH 6.8), 40% glycerol, 8% (wt/vol) SDS, 0.05 M EDTA, 0.08% bromophenol blue] without heat treatment. Separated proteins were transferred to PVDF membranes (Millipore) and nonspecific binding on the membrane was blocked with 5% BSA in PBS-T for 1 h. The membrane was incubated with a mouse antibody (Mab) 2H2 (anti-prM) and 4G2 (anti-E) as an internal control at room temperature for 3 h with shaking. HRP-conjugated anti-mouse antibody was used for detection for 1 h at room temperature with shaking. Immunoreactive proteins were visualized using WesternBright Sirius HRP substrate (Advansta) and imaged on an ImageQuant instrument (Bio-Rad). The molecular weights of the protein bands were estimated by comparison with Precision Plus Protein Dual Color Standards (Bio-Rad). The protein level were quantified by using Image J software.

2.8 RNA extraction and Real time PCR

Total RNA from cell lysate was isolated using the Trizol extraction method for cellular viral RNA quantification. 500 ng of total RNA was used for cDNA synthesis with random primers using ImProm II reverse transcription system (Promega) according to the manufacturer's instructions. 40 ng of cDNA was subjected to real-time PCR using SYBR green supermix (Bio-Rad) to quantify the intracellular viral RNA synthesis. For extracellular viral RNA quantification, vRNA in the supernatant was extracted using QIAamp Viral RNA Mini Kit (Qiagen) according to the manufacturer's instructions and subjected to real-time PCR using iTaq Universal SYBR green one step kit (Bio-Rad). Primers used for real time quantification of the viral genome has been previously described (Tay et al., 2015). Plasmid fragments containing DENV2-3295 E region genome sequences were used to generate a standard curve for quantification of viral copy number. Results were reported as absolute viral genome copy per μg RNA normalized to actin expression for cellular vRNA synthesis or absolute number of viral RNA genome copy per ml of supernatant for extracellular vRNA quantification respectively (Tay et al., 2015). The limit of detection of real-time PCR is indicated as the grey dotted line in the graph.

2.9 Generation and purification of immature dengue virus

C6/36 cells were infected with DENV-2 WT or mutants at MOI of 1 for 2 hours at 28ºC. Medium containing 2% FBS were topped up and cells were incubated for another 20 hours. The inoculums were removed and cells were washed with PBS for three times to remove the mature virus. Medium were replaced with fresh RPMI containing 2% FBS and 30 mM NH_4Cl. Virus were harvested after 48 hours incubation and PEG 8000 solution was added to have a final PEG concentration 8%. The precipitates were resuspended in NTE buffer and further purified though a 24% sucrose cushion by ultracentrifuge at 4ºC in a Beckman coulter TLA-110 fixed angle rotor

for 1.5 h at 60000 $\times g$. The viruses were harvested and subjected to 15% SDS-PAGE analysis (Yu et al., 2008).

2.10 Furin cleavage inhibition assay

Furin cleavage inhibition assay was performed in a 10 µl reaction mixture, containing 100 mM MES, 3 mM $CaCl_2$ and 120 mM NaCl at pH 6.0 (Yu et al., 2008). Approximately 10^9 copies of genome-containing immature virus particles was pre-incubated with different concentrations (0-100 µM) of luteolin or buffer without compound as negative control at 30ºC for 1 hour. Subsequently, 50 ng of furin (Abcam) was added to the reaction and further incubated for 4 hours. Before Western blotting (WB) or immunofluorescence analysis, samples were neutralized by adding 2 µl 1M Tris 8.0. For the infectivity testing using immunofluorescence assay, samples were diluted 50-fold with serum free media and used to infect BHK-21 cells for 1 h. At 24 h p.i, cells were fixed and subjected to IFA assay as described above.

2.11 Statistics analysis

Significant differences between data groups were determined by 2-tailed student *t* test analysis using GraphPad Prism software and *P* value less than 0.05 was considered statistically significant.

3. Results

3.1 Luteolin resistance maps to the prM and NS2B coding protein

To further investigate the mechanism of DENV inhibition by the flavone luteolin (Fig 1A), we set out to generate resistant virus by passaging DENV2 TSV01 strain in Huh-7 cells in the presence of increasing concentrations of luteolin (Fig. 1B). Viruses from passage 10 (P10) were assayed for the resistance phenotype by comparison of the viral titers between the mock-treated infections and luteolin-treated infections. When Huh-7 cells were infected with the multiplicity of infection (MOI) of 0.3, the viral titer yield from the P10 virus was 3-fold lower than the WT, indicating

that the reduced viral fitness of the passage 10 virus which may reflect the emergence of resistance mutations. The infectivity of the P10 generated virus in the presence or absence of 10 μM luteolin were about the same, suggesting that the P10 virus had acquired resistance to luteolin (Fig. 1C) in cell culture.

To map the mutations in the viral genome that are responsible for reduced luteolin susceptibility, the complete genome sequence of the resistant virus was obtained and compared to the wild type DENV-2 TSV01 sequence. Two nucleotide changes were identified. The sequence chromatogram showed that there was 50% C to G change at nucleotide position 674 and a 100% A to G change at nucleotide position 4473 (Fig. 1D). The nucleotide changes resulted in change of Threonine (Thr) to Arginine (Arg) at amino acid position 79 in the prM protein (T79R) which is within the 'pr' peptide and Isoleucine (Ile) to Methionine (Met) at position 114 in the NS2B protein (I114M) (Fig. 1D). These mutations were not present in the mock-treated DENV2 wild type virus cultured for 10 passages as a negative control. Sequence alignment analyzed by single nucleotide polymorphisms (SNPs) showed that T79 (100% conserved) and I114 (>98% conserved) are highly conserved among the four serotypes of DENV (Fig. 1E).

3.2 Introduction of mutations into DENV2 infectious clone and characterization of replication

Next, given that the prM T79R and NS2B I114M were present in the luteolin-treated virus but absent in the negative control virus, we tested the contribution of these two mutations to luteolin resistance by reverse genetics. The mutations were introduced, either singly as prM T79R (SM1) or NS2B I114M (SM2) or as a double mutant prM T79R-NS2B I114M (DM), into DENV2 full length infectious clone as described previously (Fig. 2A) (Tay et al., 2015; Tay et al., 2016; Zhao et al., 2015). *In vitro* transcribed genome-length RNA were transfected into C6/36 cells for generation of mutant viruses. The recombinant viruses were sequenced to verify that the mutations were introduced with no other change in the genome (data not shown).

Next we examined the infection profile of luteolin resistant mutant viruses expanded from C6/36 cells in Huh-7 cells infected at MOI 1. The growth kinetics measured by real-time quantitative RT-PCR (qPCR) showed that the replication of DM was similar to WT virus. The SM1 virus was found to be attenuated with around 13-fold (*P=0.0334) and 10-fold (P=0.0650) reduction in viral RNA replication at 24 and 48 h p.i respectively. The SM2 virus on the other hand showed faster replication than the WT virus with 3-fold increase in intracellular viral RNA level at 24 (*P=0.024) and 48 h p.i (**P=0.0057) (Fig. 2B). The infectious virus quantification by plaque assay reflected similar growth kinetics for WT and DM viruses at 24 and 48 p.i. In contrast a 6-fold reduction at 24 h p.i (**P=0.0074) and 3-fold reduction (*P=0.031) at 48 h p.i were observed for SM1 and a 2-fold increase in infective virus was observed for SM2 mutant virus at both 24 (P=0.0521) and 48 h p.i (*P=0.026) compared to WT (Fig. 2C). The plaque size of the WT and mutants were somewhat similar (Fig. 2D) indicating that plaque morphologies did not have a role in the different growth characteristics. The cellular infection levels were also reflective of the viral RNA replication as confirmed by immuno-fluorescence assay using anti-NS3 antibody (Fig. 2E). Consistent with the above data, at 48 h p.i, 60-70% cells were infected by WT and DM viruses whereas SM1 mutant showed 20-30% infectivity and SM2 mutant virus showed more than 90% infectivity.

3.3 Mutations confer resistance to luteolin

Next we performed time-of-drug addition (TODA) assay as described previously (Peng et al., 2017) to test the level of resistance to luteolin by WT and mutant viruses. DENV2 WT or mutant viruses infected Huh-7 cells were treated with 10 μM luteolin at 12 h p.i and sampled at 12, 24, 36, 60 h p.i. The intracellular and extracellular DENV genome RNA levels were monitored at the various sampled time points by real-time RT-PCR or plaque assay. The intracellular and extracellular viral RNA levels increased until 60 h p.i, for lutolin treated and untreated DENV2 WT or the mutant viruses (Supplementary Fig. 1) (Peng et al., 2017). Analysis of viral titers in

the supernatant at various time points by plaque assay showed a decrease in infective viral titer. As shown previously WT virus treated with luteolin showed ~ 90% reduction in infective virus (Peng et al., 2017) (Fig. 3A). Comparison of infective virus production of mutant viruses at 60 h.p.i following luteolin treatment in TODA assay showed different levels of inhibition, relative to untreated infection control (SM1 mutant ~60% reduction; SM2 mutant ~70% reduction and DM mutant virus ~55% reduction) (Fig. 3A).

To examine the impact of mutation on prM processing, WT or mutant virus supernatants collected at 60 h from the luteolin treated or mock treated infected cells were pelleted down by ultracentrifugation for 2 h at 32000 rpm. 10^9 genome-equivalent of WT or mutant viruses were separated by SDS-PAGE and detected by WB using 4G2 (anti-E protein Ab) and 2H2 (anti-prM protein Ab) antibodies. The WB analysis showed that the virions from both the luteolin-treated and mock-treated samples had almost the same amount of E protein for mutants and WT viruses. The mock-treated WT and mutant viruses had approximately similar levels of prM protein, suggesting that neither the SM1 nor SM2 or the combined DM viruses displayed any defect in formation of mature viruses. However with the luteolin treatment, in agreement with our previous study, the virions from the WT contained larger amounts of prM protein than mutants in the order WT>SM1>SM2>DM, indicating that the maturation process of mutant virus particles secreted in the supernatants from luteolin treatment were more complete (Fig. 3B). Collectively, these results show that the mutations tested confer some level of resistance to luteolin.

3.4 The prM T79R mutation contributes to resistance at the step of virus maturation

Since NS2B is not packaged in an infected virion we wanted to examine the in vitro furin cleavage of prM on WT and mutant viruses in order to understand the basis of the luteolin inhibition. Approximately 10^9 genome copies of immature WT virus particles propagated from C6/36 cells using RPMI 1640 medium containing 30 mM NH_4Cl following PEG 8000

precipitation and sucrose cushion purification (Yu et al., 2008) were pre-incubated with various concentrations (5, 10, 25, 50, 100 μM) of luteolin for 1 h and further incubated with exogenous furin for 4 h at 30°C in buffer containing 100 mM MES, 3 mM $CaCl_2$ and 120 mM NaCl at pH 6.0, after which the protein composition of virus particles were analyzed by WB. The prM protein level were quantified by Image J and E protein was used as a control. A dose dependent cleavage of prM was observed and the maximal inhibition of the cleavage was achieved at a concentration of 50 μM with ~100% reduction (Fig. 4A and B).

After validation of the exogenous furin cleavage assay we proceeded to investigate whether treatment of immature mutant virions with luteolin (50 μM) followed by exogenous furin treatment could cleave prM and restore mutant virus infectivity (Fig. 4C and D). For the immature virus control (without furin or luteolin), a prominent prM band was detected by WB in both WT and mutants samples, indicating that the immature viruses were successfully made. After exposure to 50 ng of furin the level of prM detection by WB was drastically reduced for WT and mutant immature virus particles. However when the immature WT or mutant viruses were pre-treated with 50 μM luteolin and then subjected to furin cleavage, the levels of prM protein in WT or SM2 immature viruses were almost similar to the input immature virus (without furin or luteolin treatment). The level of prM in the SM1 mutant immature virus was slightly reduced (~73% reduction) compared to the input level suggesting that this mutation was less susceptible to luteolin. However, the amount of prM protein in the luteolin treated DM immature particles with 87% reduction were similar to furin only treated virus control suggesting that the DM immature virus is not susceptible to luteolin and can be readily cleaved by furin (Fig. 4C and D). Thus luteolin is able to block the prM cleavage of WT, and SM2 immature viruses effectively and SM1 marginally but not DM immature virus which is not susceptible to luteolin inhibition.

The biological activity of the *in vitro* furin-treated virus samples were tested in infection assays and infectivity assessed by immunofluorescence assay using 4G2 (anti-E protein) and 3F8 (anti-

NS3 protein). BHK-21 cells were infected with samples derived from the furin cleavage assay and incubated for 24 h. Firstly the purified immature WT and mutant viruses showed no infection at all confirming that they were non-infectious. With 50 ng of furin addition, the viral infectivity was dramatically increased for all viruses (~50-60% cells infected) due to cleavage of prM to M by furin. However, with 50 μM luteolin treatment, the infectivity was virtually abolished in the WT and SM2 samples in agreement with the prM detection by WB following SDS-PAGE. On the other hand, the viral infectivity of DM immature virus treated with lueolin and furin was in the range of 30-40% while SM1 immature virus showed 5-10%infectivity (Fig. 4E). Together the data suggests that prM T79R mutantion was less sensitive to luteolin inhibition than WT.

4. Discussion

The escalation of dengue cases globally coupled with the slow uptake of the only licensed tetravalent dengue vaccine due to lack of complete protection, as well as the lack of any promising directly acting antiviral candidates in the development pipeline (Low et al., 2017) led to the search for solution in the TCM pharmacopoeia. Luteolin, a widely-studied flavone component isolated from *Viola yedoensis Makino* a TCM herbal medicine used as a "heat-clearing" panacea, was found to be an effective agent against DENV mainly through inhibition of the cellular proprotein convertase furin (Peng et al., 2017). It is well-known that the lack of fidelity of RNA polymerase leads to emergence of viral quasispecies during replication that can lead to expansion drug-resistant strains during antiviral treatment. However, host-based antivirals are thought to possess the advantage of having a high genetic barrier for generation of escape mutants. Since *in vitro* enzyme inhibition studies showed that luteolin can inhibit both the host furin and viral NS3 protease albeit not with equal potency, resistant mutants were generated in cell culture to provide further insights into the mechanism of action of the drug which could influence the specific use of TCM medicines in dengue fever.

DENV2 with reduced susceptibility to luteolin appeared in the 10^{th} passage in cell culture and luteolin sensitivity determinant factors mapped to the prM and NS2B coding region of genome. The sequence analysis showed that 100% on the resistant mutants carried the I114M change in NS2B while the mutation T79R at prM showed a 50% frequency. Coincidently, these two mutations indirectly corresponded to our previous finding that luteolin was an uncompetitive inhibitor of host protease furin as well as a weak noncompetitive inhibitor of viral protease NS2B-NS3. Given that the Ki for furin was lower than the dengue protease we further interrogated the mutations by reverse engineering the mutations into a DENV 2 infectious clone derived from a clinical strain in Singapore (Low et al., 2006) in order to understand the contribution of the two amino acids substitution to the loss of compound susceptibility.

The single mutation SM1 (prM T79R) was found attenuated and showed a lower replication capacity compared to WT. Maturation of DENV during egress occurs through furin cleavage after 87-RXKR-91 motif (Fig.1E) thereby removing the N-terminal 91 "pr" and leaving the ectodomain (residues 92 to 130) and C-terminal transmembrane region (residues 131 to 166) to form the M protein on the virion surface (Li et al., 2008). The Pr peptide comprises seven mostly antiparallel β-strands and prM T79R is located at the end of seventh β-strand (g_{pr}) (Li et al., 2008). The Pr peptide is also stabilized by three conserved disulfide bridges and one of them is between Cys 45 and Cys 80 (Li et al., 2008). Since the T79R mutation is adjacent to the conserved disulfide bridge it is possible that the Arg side-chain of the mutant may disrupt the interaction between furin and the immature prM thereby reducing its cleavage efficiency. It is also possible the newly introduced mutation may interact with E protein and make it less accessible for furin cleavage in the highly finetuned pH in the *trans* Golgi compartment (Li et al., 2008; Nemesio and Villalain, 2014).

The single mutation SM2 (NS2B I114M) showed increased replicative fitness and was found in nearly 100% of the escape mutants based on sequence analysis suggesting that this may the first

escape mutation to appear as a consequence of increasing lueolin concentration during the 10 passages. Why a luteolin escape mutant with increased fitness should occur through a mutation in NS2B that forms a membrane anchor and cofactor for NS3 protease is unclear, although Leu-to-Met may increase the hydrophobicity of NS2B and further stabilize its membrane association (Li et al., 2014; Li et al., 2015; Luo et al., 2015) (Erbel et al., 2006). In the double mutant (DM) virus replication fitness is restored to WT levels in comparison with attenuation seen in SM1 and increased fitness noted in SM2. Compared to WT both SM1 & SM2 showed higher furin cleavage activity as measured by the level of prM (Fig. 3B) in the TODA assay. A previous study in a related flavivirus has suggested that cleavage of prM in the lumen of the endoplasmic reticulum by signal peptidase and the subsequent secretion of E/prM spike heterodimer is under control of a cytoplasmic cleavage catalyzed by the activity of the viral protease NS3 (Lobigs, 1993). Furthermore it has been shown that DENV NS3 interacts with fatty acid synthase (FASN) to meet the lipid load required for establishing viral replication centers and production of virion particles (Heaton et al., 2010). It is also conceivable that the increased fitness of SM2 may result from membrane remodeling that may make the resulting virion particle slightly more susceptible to furin cleavage in the presence of luteolin in the TODA assay. For further insights into the luteolin binding sites that lead to inhibition of furin cleavage, the ability of purified furin to cleave immature WT and mutant viruses in the presence or absence of 50μM luteolin was assessed by WB and infection analysis. The immature DM virus was able to completely escape the inhibitory effect of the drug and was activated to almost the same level as with furin alone. On the other hand the furin cleavage of WT and SM2 immature viruses were blocked by 50μM luteolin, while SM1 was still slightly susceptible to furin cleavage. Taken together the data suggests that any membrane remodeling or change of the membrane anchorage of the NS2B protein that may have been introduced by SM2 mutation alone does not result in escape from

luteolin inhibiton although the TODA assay shows some level of inhibition suggesting that luteolin is inhibiting furin.

Furin cleavage is considered a potential drug target for treatment of several pathologies including infectious diseases(Seidah and Prat, 2012). An extensive drug discovery campaign identified dicoumarol compounds inhibit the activity of furin (Komiyama et al., 2009). Although no crystal structure are available for binding of flavones or dicoumarols a recent study with small molecule inhibitors ((Dahms et al., 2017) revealed that their binding alters the critical substrate binding pockets S1 and S4 that may lead to inhibition of the cleavage activity. Further structural studies are required to fully understand the interface between furin and flaviviral prM but the current study suggests that compounds based on flavones like luteolin can form starting point for pan-flavivirus development.

In summary dengue fever caused by dengue virus (DENV) infection transmitted by mosquitoes is a major public health threat to almost half of the world's population, particularly in tropical and subtropical countries where outbreaks occur regularly. Unfortunately, there is no effective vaccine or approved medicine for DENV infection prevention. The widespread use of TCM herbs in Asia prompted a systematic study that identified luteolin, a component in TCM herbs that are "heat clearing" for fever reduction, as an inhibitor of all four DENV serotypes. We identified luteolin-escape mutants that mapped to the viral prM and NS2B proteins that are associated with the viral maturation step. Since flaviviral infections are acute, short-course antiviral treatment targeting furin could be an attractive approach.

Acknowledgments

We thank colleagues at the Duke-NUS medical school for technical support and valuable commends during the course of this study. We also thank Dr Jiaqi Wang from Shee Mei Lok's lab for good suggestions on purification of immature virus and furin cleavage assay.

This project was partially supported by the funding Science & Technology Planning Project of Guangdong Province of China (No. 2013A020229007), Innovative program of State Key Laboratory of Virology (No. 2016KF001), Science & Technology Planning Project of Guangzhou (No. 2018-1002-SF-0433)

Figure legends

Figure 1. Selection and sequencing of luteolin-resistant DENV-2 mutants.

A, Chemical structure of luteolin. B, Scheme for selection of luteolin-resistant DENV-2 mutant virus. P1-P3 were selected at 5 μM luteolin, P4-P6 were selected at 10 μM luteolin, P7-P9 were selected at 15 μM luteolin, P10-P13 were selected at 20 μM luteolin. Viral titer was determined by plaque assay. C, Resistance analysis. Huh-7 cells were infected with P10 mock-treated or luteolin treated viruses at MOI 0.3 for 1 h. Inoculums were replaced with fresh medium containing 10 μM luteolin or 0.05% DMSO as negative control. At 48 h p.i., supernatants were collected. BHK-21 cell monolayers were infected with supernatants at 100-fold dilution and stained with crystal violet at 5 days p.i. Resistance is quantified by comparison of the viral titers from the luteolin-treated infection with the untreated infections. D, The P10 viral RNA was extracted for whole-genome sequencing. The mutations were showed in the chromatograms. E, Amino sequence alignment of the DENV prM and NS2B protein, illustrating the location of mutation (red) and furin cleavage sequence (purple). The sequences of DENV2 (TSV01), DENV-1, DENV-2, DENV-3, DENV-4 are derived from the sequences with GenBank accession number AY037116, EU081230, EU081177, EU081190, GQ398256, respectively.

Figure 2. Replication profile of luteolin-resistant mutants in Huh-7 cells.

A, Schematics of DENV2 3295 infectious clone used in this study showing the introduction of prM T79R (cross star) and NS2B I114M mutation (pentagram). B, Huh-7 cells were infected with DENV WT or luteolin resistant mutants at MOI 1. Intracellular viral RNA level was monitored by real-time RT-PCR at 6, 12, 24, 48 h post-infection. The gray dotted line in the graph represents the limit of detection of real-time PCR. C, Virus titers in the supernatants from 24 and 48 h post-infection were determined by standard BHK-21 plaque assay. Data are shown as the mean ± SD from two independent experiments. D, Plaque morphologies of WT and mutants at 24

h post-infection with 1000-fold dilution. E, IFA images showing NS3 (Alexa 594) staining of infected cells and the percentage infection at 48 h post-infection. The asterisk indicates a difference that is statistically significant (*$P < 0.05$, **$P < 0.01$).

Figure 3. Analysis for resistance of luteolin on DENV2 WT and mutant viruses.

A, Huh-7 cells were infected with DENV-2 WT or mutant viruses at a MOI of 1 prior to the addition of 10 μM of luteolin at 12 h after infection. Supernatants were collected at 60 h p.i and virus titers were measured by standard BHK-21 plaque assay. The error bar indicates the standard deviation of three independent experiments. The asterisk indicates a difference that is statistically significant (*P < 0.05, **P < 0.01). B, Supernatants collected at 60 h after infection were concentrated and subjected to Western blot analysis using antibodies 4G2 and 2H2 directed toward dengue viral E and prM protein, respectively. The asterisk indicates a difference that is statistically significant (*$P < 0.05$, **$P < 0.01$)

Figure 4. Analysis of luteolin inhibition of cleavage of prM in WT or mutant viruses

A, Purified immature DENV-2 WT virus particles were pre-incubated with different concentrations (0-100 μM) of luteolin at 30°C for 1 h before the addition of 50 ng of furin. After further incubation for 4 h, protein compositions were analyzed by Western blot using antibodies 4G2 and 2H2 directed toward viral E and prM protein, respectively. B and D, Bar graph for the quantitative comparison among protein levels. The signal intensities of a protein band scanned from images derived from two independent experiments and quantified using image J software. The values of prM protein level were normalized to those of E protein and then plotted was relative protein levels. Reduction % = (with luteolin-with furin only) / (immature virus only- with furin only) *100%. C, Purified immature DENV-2 WT or mutant virus particles were incubated with 50 μM luteolin and furin. Protein compositions were analyzed by western blot as described above. E, Then infectivity of immature dengue viruses with or without furin cleavage was

analyzed by immunofluorescence assay. Samples were diluted with 50-fold and used to infect BHK-21 cells. Cells were fixed at 24 h p.i. IFA images showing E (Alexa 488) and NS3 (Alexa 594) staining of infected cells and the percentage infection after furin cleavage.

Reference

Aguiar M, H.S., Stollenwerk N., 2017. Consider stopping dengvaxia administration without immunological screening. Expert Review of Vaccines 16, 301-302.

Bhatt, S., Gething, P.W., Brady, O.J., Messina, J.P., Farlow, A.W., Moyes, C.L., Drake, J.M., Brownstein, J.S., Hoen, A.G., Sankoh, O., Myers, M.F., George, D.B., Jaenisch, T., Wint, G.R., Simmons, C.P., Scott, T.W., Farrar, J.J., Hay, S.I., 2013. The global distribution and burden of dengue. Nature 496, 504-507.

Brady, O.J., Gething, P.W., Bhatt, S., Messina, J.P., Brownstein, J.S., Hoen, A.G., Moyes, C.L., Farlow, A.W., Scott, T.W., Hay, S.I., 2012. Refining the global spatial limits of dengue virus transmission by evidence-based consensus. PLoS Negl Trop Dis 6, e1760.

Christenbury, J.G., Aw, P.P., Ong, S.H., Schreiber, M.J., Chow, A., Gubler, D.J., Vasudevan, S.G., Ooi, E.E., Hibberd, M.L., 2010. A method for full genome sequencing of all four serotypes of the dengue virus. J Virol Methods 169, 202-206.

Collins, T.J., 2007. ImageJ for microscopy. Biotechniques 43, 25-30.

Dahms, S.O., Jiao, G.S., Than, M.E., 2017. Structural Studies Revealed Active Site Distortions of Human Furin by a Small Molecule Inhibitor. ACS Chem Biol 12, 1211-1216.

Erbel, P., Schiering, N., D'Arcy, A., Renatus, M., Kroemer, M., Lim, S.P., Yin, Z., Keller, T.H., Vasudevan, S.G., Hommel, U., 2006. Structural basis for the activation of flaviviral NS3 proteases from dengue and West Nile virus. Nat Struct Mol Biol 13, 372-373.

Garcia-Blanco, M.A., Vasudevan, S.G., Bradrick, S.S., Nicchitta, C., 2016. Flavivirus RNA transactions from viral entry to genome replication. Antiviral Res 134, 244-249.

Hadinegoro, S.R., Arredondo-Garcia, J.L., Capeding, M.R., Deseda, C., Chotpitayasunondh, T., Dietze, R., Muhammad Ismail, H.I., Reynales, H., Limkittikul, K., Rivera-Medina, D.M., Tran, H.N., Bouckenooghe, A., Chansinghakul, D., Cortes, M., Fanouillere, K., Forrat, R., Frago, C., Gailhardou, S., Jackson, N., Noriega, F., Plennevaux, E., Wartel, T.A., Zambrano, B., Saville, M., Group, C.-T.D.V.W., 2015. Efficacy and Long-Term Safety of a Dengue Vaccine in Regions of Endemic Disease. N Engl J Med 373, 1195-1206.

Halstead, S.B., 2007. Dengue. Lancet 370, 1644-1652.

Heaton, N.S., Perera, R., Berger, K.L., Khadka, S., Lacount, D.J., Kuhn, R.J., Randall, G., 2010. Dengue virus nonstructural protein 3 redistributes fatty acid synthase to sites of viral replication and increases cellular fatty acid synthesis. Proc Natl Acad Sci U S A 107, 17345-17350.

Komiyama, T., Coppola, J.M., Larsen, M.J., van Dort, M.E., Ross, B.D., Day, R., Rehemtulla, A., Fuller, R.S., 2009. Inhibition of furin/proprotein convertase-catalyzed surface and intracellular processing by small molecules. J Biol Chem 284, 15729-15738.
Kuhn, R.J., Zhang, W., Rossmann, M.G., Pletnev, S.V., Corver, J., Lenches, E., Jones, C.T., Mukhopadhyay, S., Chipman, P.R., Strauss, E.G., Baker, T.S., Strauss, J.H., 2002. Structure of dengue virus: implications for flavivirus organization, maturation, and fusion. Cell 108, 717-725.
Li, J., Lim, S.P., Beer, D., Patel, V., Wen, D., Tumanut, C., Tully, D.C., Williams, J.A., Jiricek, J., Priestle, J.P., Harris, J.L., Vasudevan, S.G., 2005. Functional profiling of recombinant NS3 proteases from all four serotypes of dengue virus using tetrapeptide and octapeptide substrate libraries. J Biol Chem 280, 28766-28774.
Li, K., Phoo, W.W., Luo, D., 2014. Functional interplay among the flavivirus NS3 protease, helicase, and cofactors. Virol Sin 29, 74-85.
Li, L., Lok, S.M., Yu, I.M., Zhang, Y., Kuhn, R.J., Chen, J., Rossmann, M.G., 2008. The flavivirus precursor membrane-envelope protein complex: structure and maturation. Science 319, 1830-1834.
Li, Y., Li, Q., Wong, Y.L., Liew, L.S., Kang, C., 2015. Membrane topology of NS2B of dengue virus revealed by NMR spectroscopy. Biochim Biophys Acta 1848, 2244-2252.
Lobigs, M., 1993. Flavivirus premembrane protein cleavage and spike heterodimer secretion require the function of the viral proteinase NS3. Proc Natl Acad Sci U S A 90, 6218-6222.
Low, J.G., Ooi, E.E., Tolfvenstam, T., Leo, Y.S., Hibberd, M.L., Ng, L.C., Lai, Y.L., Yap, G.S., Li, C.S., Vasudevan, S.G., Ong, A., 2006. Early Dengue infection and outcome study (EDEN) - study design and preliminary findings. Ann Acad Med Singapore 35, 783-789.
Low, J.G., Ooi, E.E., Vasudevan, S.G., 2017. Current Status of Dengue Therapeutics Research and Development. J Infect Dis 215, S96-S102.
Luo, D., Vasudevan, S.G., Lescar, J., 2015. The flavivirus NS2B-NS3 protease-helicase as a target for antiviral drug development. Antiviral Res 118, 148-158.
McBride WJH, V.S., 1995. Relationship of a dengue 2 isolate from Townsville, 1993, to international isolates. CommDis Intelligence 19, 522-523.
Modis, Y., Ogata, S., Clements, D., Harrison, S.C., 2004. Structure of the dengue virus envelope protein after membrane fusion. Nature 427, 313-319.
Moreland, N.J., Susanto, P., Lim, E., Tay, M.Y., Rajamanonmani, R., Hanson, B.J., Vasudevan, S.G., 2012. Phage display approaches for the isolation of monoclonal antibodies against dengue virus envelope domain III from human and mouse derived libraries. Int J Mol Sci 13, 2618-2635.
Nemesio, H., Villalain, J., 2014. Membranotropic regions of the dengue virus prM protein. Biochemistry 53, 5280-5289.
Peng, M., Watanabe, S., Chan, K.W.K., He, Q., Zhao, Y., Zhang, Z., Lai, X., Luo, D., Vasudevan, S.G., Li, G., 2017. Luteolin restricts dengue virus replication through inhibition of the proprotein convertase furin. Antiviral Res 143, 176-185.
Reid, D.W., Campos, R.K., Child, J.R., Zheng, T., Chan, K.W.K., Bradrick, S.S., Vasudevan, S.G., Garcia-Blanco, M.A., Nicchitta, C.V., 2018. Dengue virus selectively annexes endoplasmic reticulum-associated translation machinery as a strategy for co-opting host cell protein synthesis. J Virol.
Richter, M.K., da Silva Voorham, J.M., Torres Pedraza, S., Hoornweg, T.E., van de Pol, D.P., Rodenhuis-Zybert, I.A., Wilschut, J., Smit, J.M., 2014. Immature dengue virus is infectious in human immature dendritic cells via interaction with the receptor molecule DC-SIGN. PLoS One 9, e98785.

Rodenhuis-Zybert, I.A., van der Schaar, H.M., da Silva Voorham, J.M., van der Ende-Metselaar, H., Lei, H.Y., Wilschut, J., Smit, J.M., 2010. Immature dengue virus: a veiled pathogen? PLoS Pathog 6, e1000718.
Seema, Jain, S.K., 2005. Molecular mechanism of pathogenesis of dengue virus: Entry and fusion with target cell. Indian J Clin Biochem 20, 92-103.
Seidah, N.G., Prat, A., 2012. The biology and therapeutic targeting of the proprotein convertases. Nat Rev Drug Discov 11, 367-383.
Tay, M.Y., Saw, W.G., Zhao, Y., Chan, K.W., Singh, D., Chong, Y., Forwood, J.K., Ooi, E.E., Gruber, G., Lescar, J., Luo, D., Vasudevan, S.G., 2015. The C-terminal 50 amino acid residues of dengue NS3 protein are important for NS3-NS5 interaction and viral replication. J Biol Chem 290, 2379-2394.
Tay, M.Y., Smith, K., Ng, I.H., Chan, K.W., Zhao, Y., Ooi, E.E., Lescar, J., Luo, D., Jans, D.A., Forwood, J.K., Vasudevan, S.G., 2016. The C-terminal 18 Amino Acid Region of Dengue Virus NS5 Regulates its Subcellular Localization and Contains a Conserved Arginine Residue Essential for Infectious Virus Production. PLoS Pathog 12, e1005886.
Yu, I.M., Zhang, W., Holdaway, H.A., Li, L., Kostyuchenko, V.A., Chipman, P.R., Kuhn, R.J., Rossmann, M.G., Chen, J., 2008. Structure of the immature dengue virus at low pH primes proteolytic maturation. Science 319, 1834-1837.
Zhao, Y., Soh, T.S., Zheng, J., Chan, K.W., Phoo, W.W., Lee, C.C., Tay, M.Y., Swaminathan, K., Cornvik, T.C., Lim, S.P., Shi, P.Y., Lescar, J., Vasudevan, S.G., Luo, D., 2015. A crystal structure of the Dengue virus NS5 protein reveals a novel inter-domain interface essential for protein flexibility and virus replication. PLoS pathogens 11, e1004682.

Figure 1

A

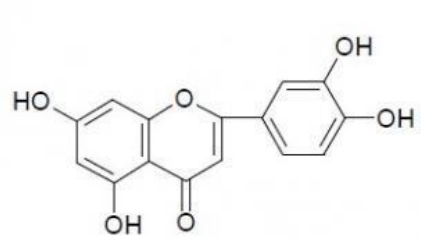

B

Selection of luteolin-resistant DENV-2

P1-P3: 5 μM luteolin

↓

P4-P6: 10 μM luteolin

↓

P7-P9: 15 μM luteolin

↓

P10-P13: 20 μM luteolin

↓

Plaque quantification

C

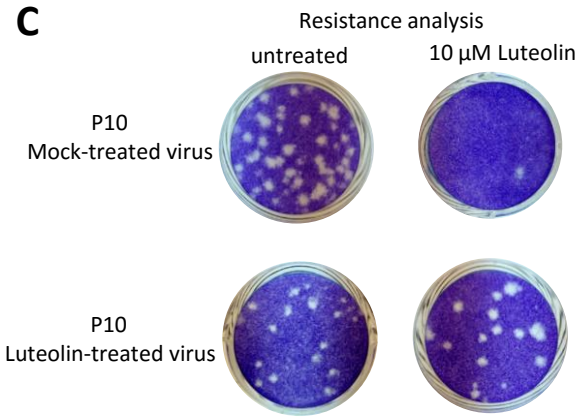

D

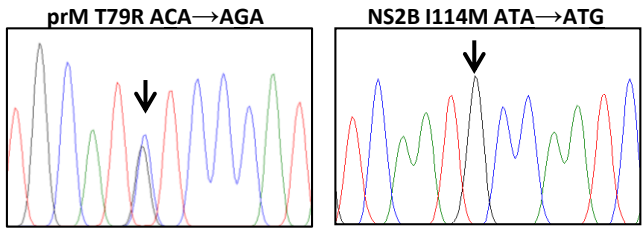

E

PrM

	71	T79R ↓	Furin cleavage sequence	100
DENV-2(TSV01)	TSTWVTYG	T	CTATGEHRREKRSVALVPHVG	
DENV-1	TDTWVTYG	T	CSQTGEHRRDKRSVALAPHVG	
DENV-2	TSTWVTYG	T	CTATGEHRREKRSVALVPHVG	
DENV-3	TSTWVTYG	T	CNQAGEHRRDKRSVALAPHVG	
DENV-4	TSTWVMYG	T	CTQNGERRREKRSVALTPHSG	

NS2B

	101	I114M ↓	130
DENV-2(TSV01)	TGLLVISGLFPAS	I	PITAAAWYLWEVKKQR
DENV-1	ATLLAVSGVYPLS	I	PATLFVWYFWQKKKQR
DENV-2	TGLLVISGLFPVS	I	PITAAAWYLWEVKKQR
DENV-3	TALLIVSGIFPYS	I	PATLLVWHTWQKQTQR
DENV-4	LALITVSGLYPLA	I	PVTMALWYIWQVKTQR

F

Figure 2

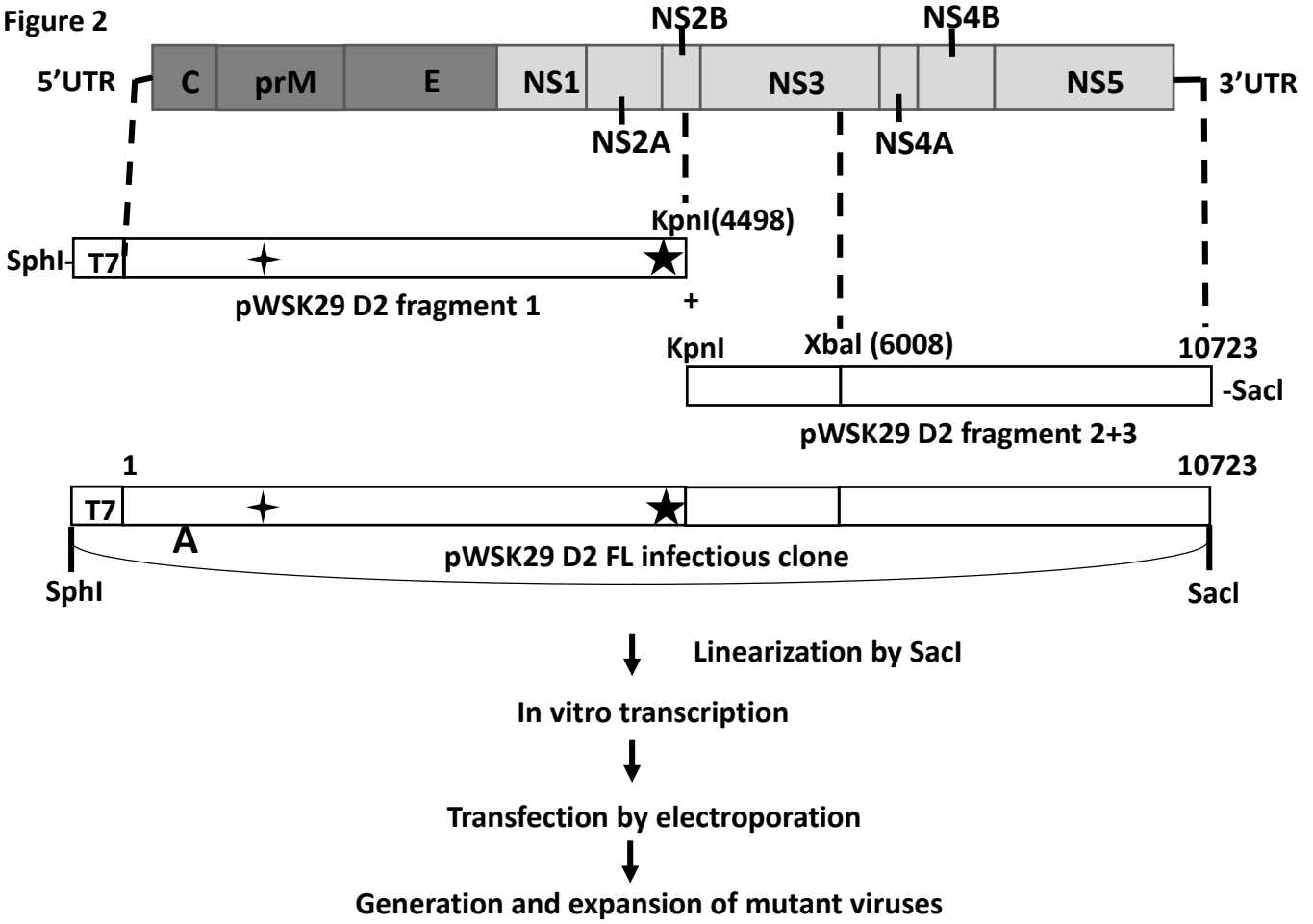
NS2B
NS4B
5'UTR
C
prM
E
NS1
NS3
NS5
3'UTR
NS2A
NS4A
KpnI(4498)
SphI-
T7
pWSK29 D2 fragment 1
+
KpnI
XbaI (6008)
10723
-SacI
pWSK29 D2 fragment 2+3
1
10723
T7
A
pWSK29 D2 FL infectious clone
SphI
SacI
Linearization by SacI
In vitro transcription
Transfection by electroporation
Generation and expansion of mutant viruses

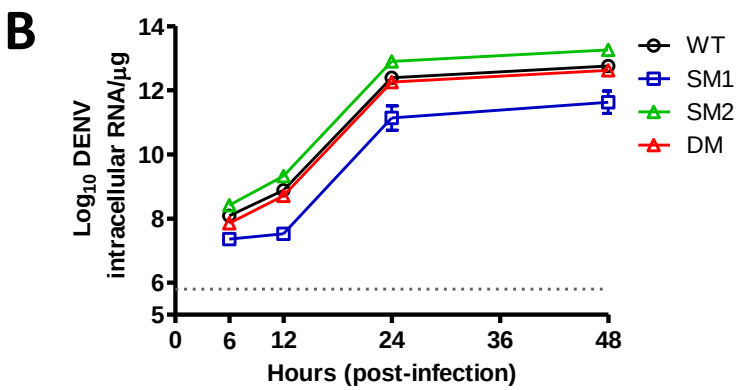
B
Log10 DENV intracellular RNA/µg
14
12
10
8
6
5
0
6
12
24
36
48
Hours (post-infection)
WT
SM1
SM2
DM

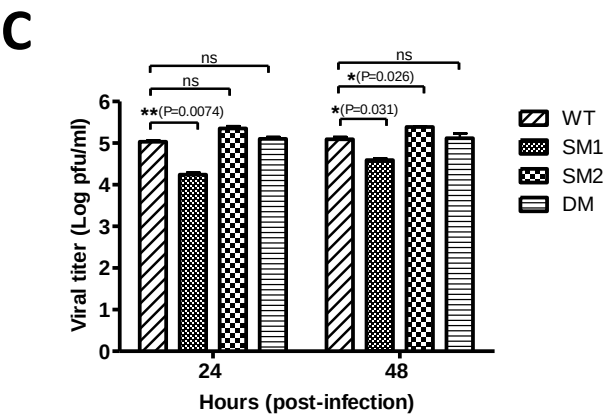
C
Viral titer (Log pfu/ml)
6
5
4
3
2
1
0
ns
ns
**(P=0.0074)
*(P=0.026)
*(P=0.031)
24
48
Hours (post-infection)
WT
SM1
SM2
DM

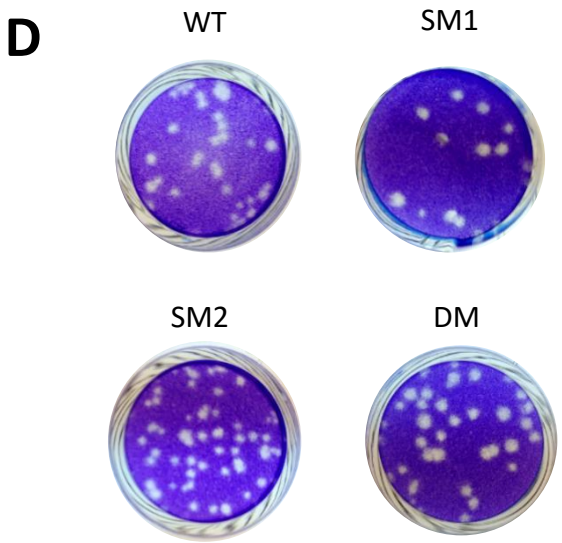
D
WT
SM1
SM2
DM

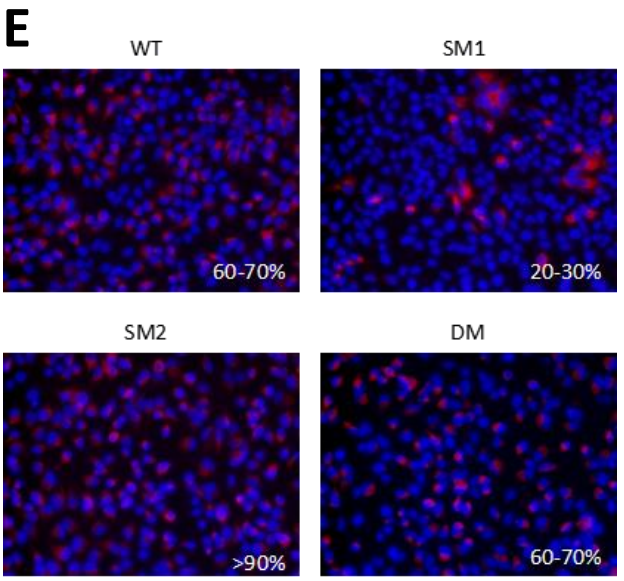
E
WT
SM1
60-70%
20-30%
SM2
DM
>90%
60-70%

Figure 3

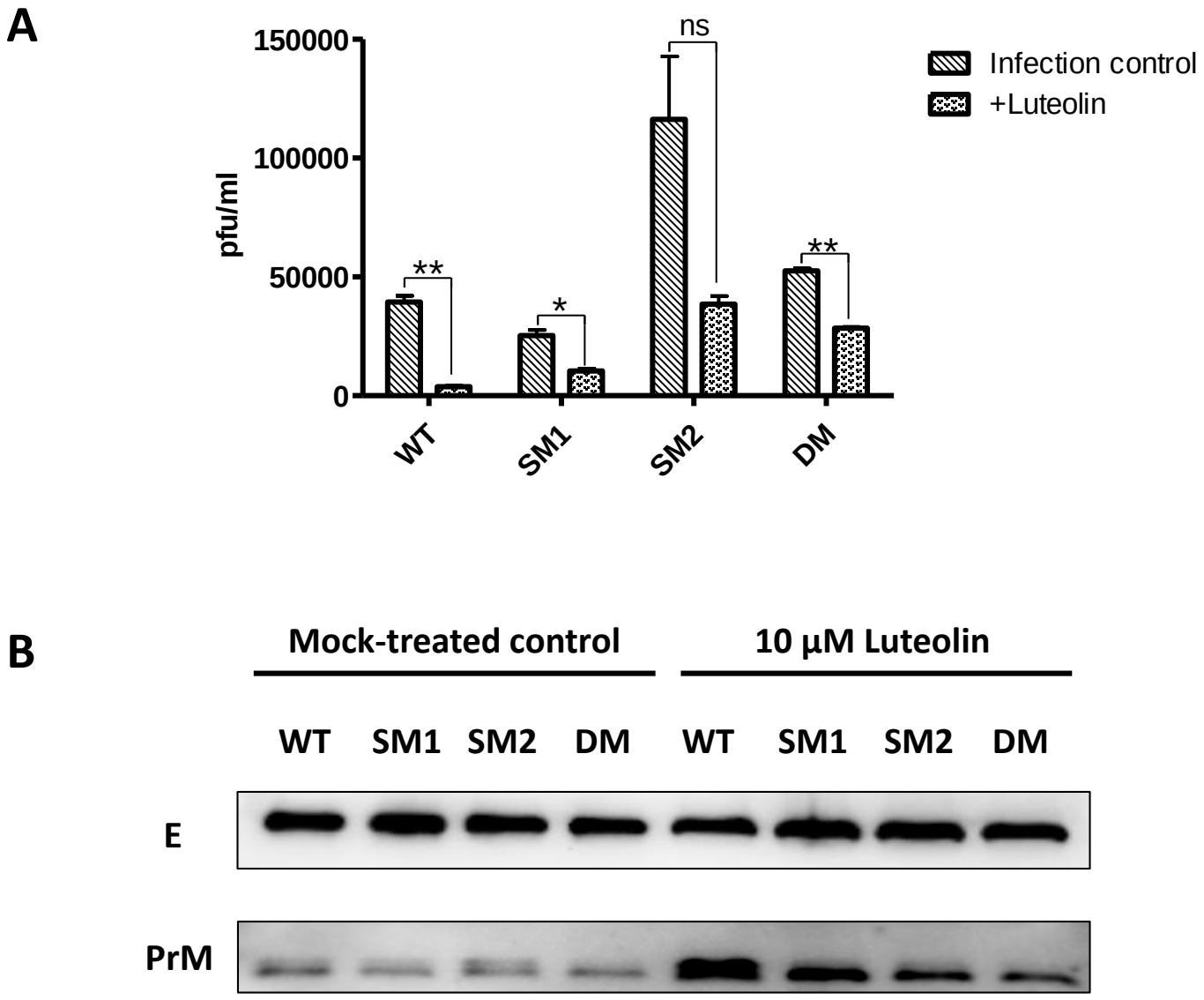
A
150000
100000
50000
0
pfu/ml
**
*
ns
**
WT
SM1
SM2
DM
Infection control
+Luteolin
B
Mock-treated control
10 μM Luteolin
WT
SM1
SM2
DM
WT
SM1
SM2
DM
E
PrM

Figure 4

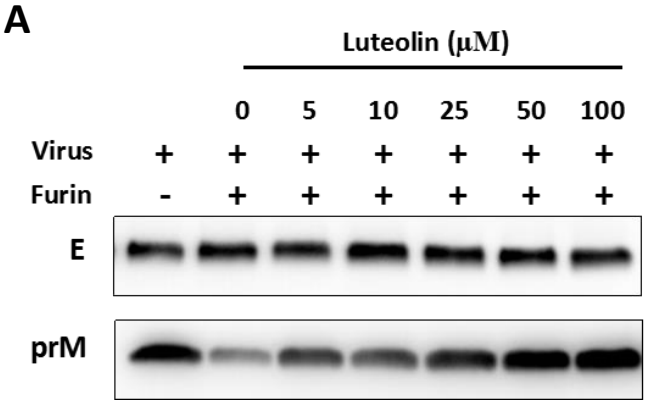
A
Luteolin (μM)
0 5 10 25 50 100
Virus + + + + + + +
Furin - + + + + + +
E
prM

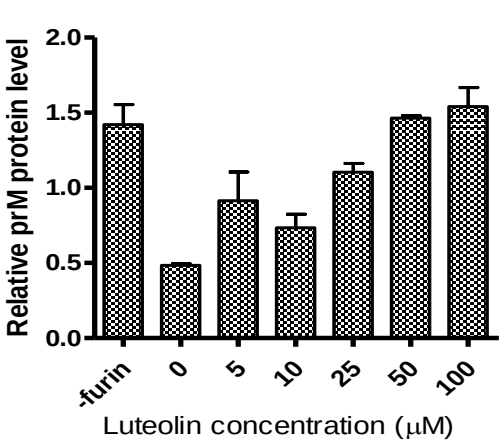
B
Relative prM protein level
2.0
1.5
1.0
0.5
0.0
-furin 0 5 10 25 50 100
Luteolin concentration (μM)

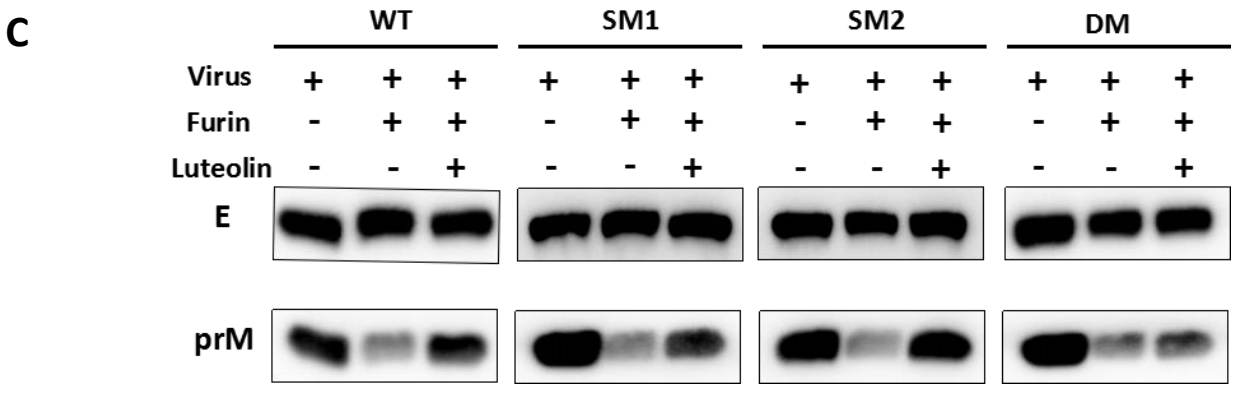
C
WT SM1 SM2 DM
Virus + + + + + + + + + + + +
Furin - + + - + + - + + - + +
Luteolin - - + - - + - - + - - +
E
prM

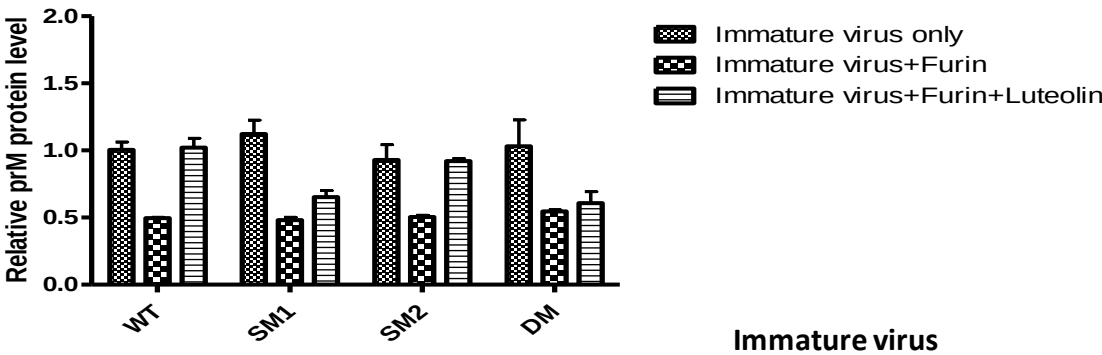
D
Relative prM protein level
2.0
1.5
1.0
0.5
0.0
WT SM1 SM2 DM
Immature virus only
Immature virus+Furin
Immature virus+Furin+Luteolin

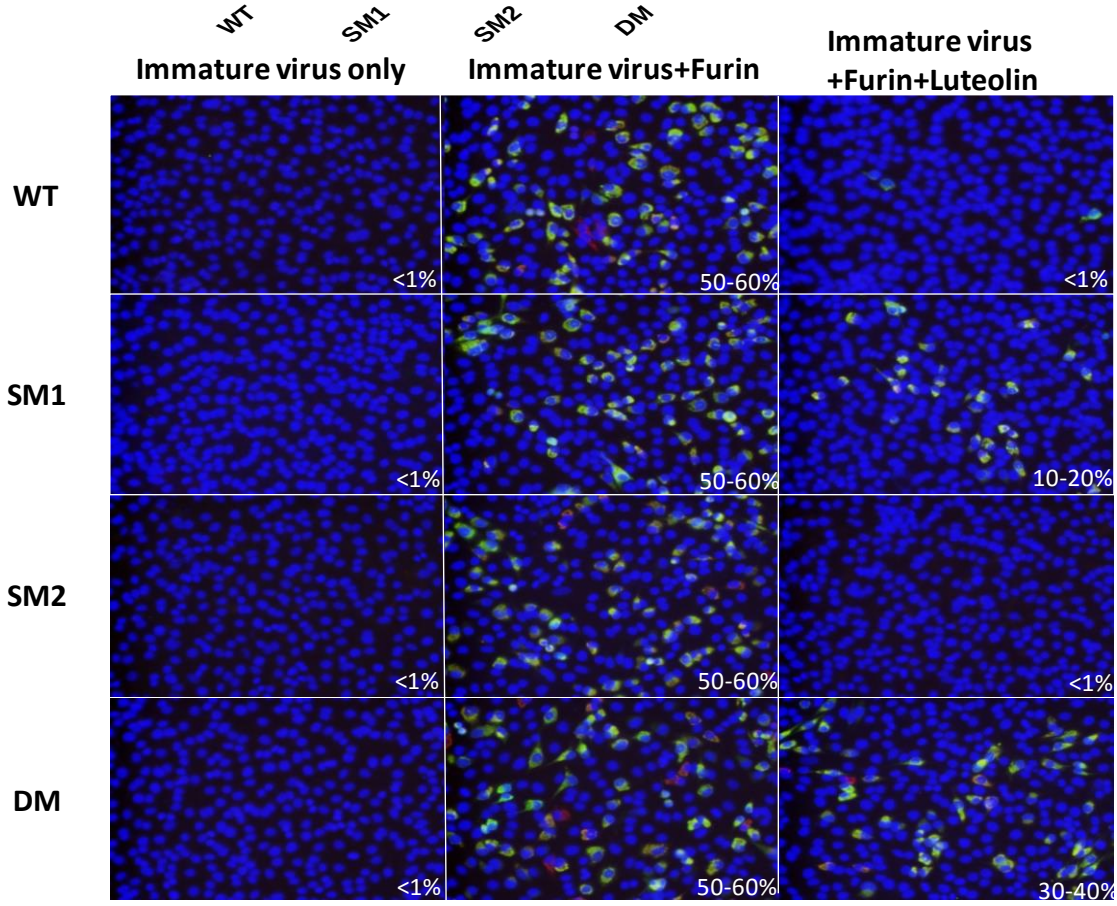
E
Immature virus only
Immature virus+Furin
Immature virus +Furin+Luteolin
WT
SM1
SM2
DM
<1%
50-60%
<1%
<1%
50-60%
10-20%
<1%
50-60%
<1%
<1%
50-60%
30-40%

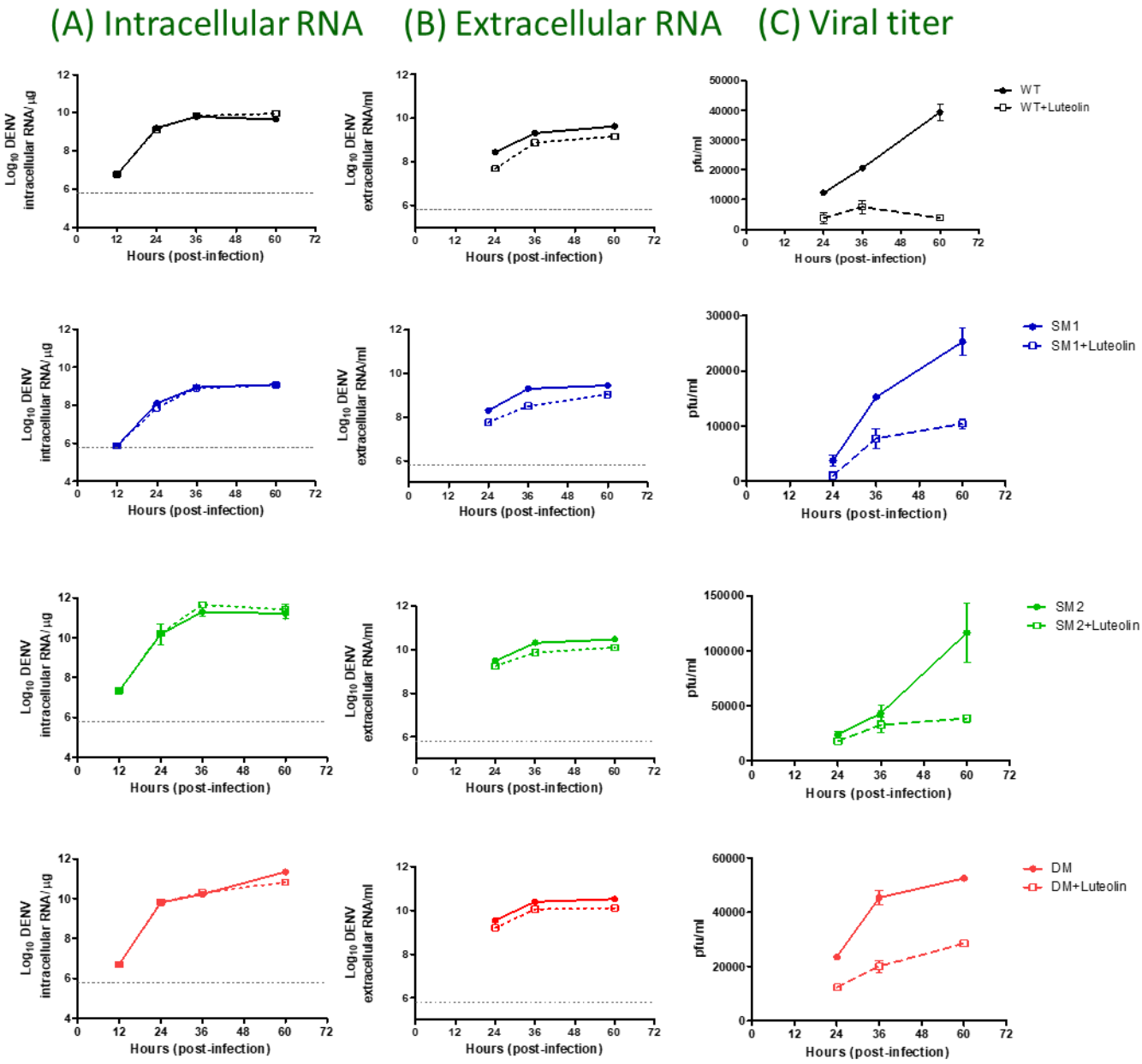

Fig. S1. Analysis for resistance of luteolin on DENV2 WT and mutant viruses. (A) Huh-7 cells were infected with DENV-2 WT or mutant viruses at a MOI of 1 prior to the addition of 10 μM of luteolin at 12 h after infection. Cells were lysed at 12, 24, 36, 60 h p.i and RNA was extracted by Trizol. Absolute number of intracellular viral RNA genome copy was measured by real time RT-PCR. (B)Simultaneously, supernatants were collected and virus titers were measured by real time RT-PCR to determine the absolute number of secreted viral RNA genome copy. (C)The infectious virus particles levels in the supernatants from 24 to 60 h p.i were determined by standard BHK-21 plaque assay. The limit of detection of real-time PCR is indicated as the grey dotted line in the graph.